Features of Lateral Particle Distributions in the Core of High-Energy Extensive Air Showers from a Multifractal Moments Analysis

A. Haungs, J. Kempa, H.-J. Mathes,
H. Rebel, J. Wentz
Institut für Kernphysik

Forschungszentrum Karlsruhe
Technik und Umwelt

Wissenschaftliche Berichte

FZKA 5618

Features of Lateral Particle Distributions in the Core of High-Energy Extensive Air Showers from a Multifractal Moments Analysis

A. Haungs, J. Kempa*, H.-J. Mathes, H. Rebel, J. Wentz

Institut für Kernphysik
*Permanent Address: University of Lodz, Lodz, Poland

Abstract

The central detector of the KASCADE (KArlsruhe Shower Core and Array DEtector) experiment is able to observe the density distributions of the main Extensive Air Shower (EAS) components in the shower core. In particular the muon component is measured precisely by large-area position-sensitive multiwire proportional chambers (MWPC), installed below the hadron calorimeter (1000 g/cm^2 Fe). Using the method of a multifractal moments analysis, applied to simulated data as being 'observed' by the MWPC, differences of the EAS lateral distributions for different type of primaries are revealed. First results from data measured with the MWPC are communicated.

Eigenschaften von Lateralverteilungen der Teilchen im Zentrum hochenergetischer ausgedehnter Luftschauer durch die Analyse multifraktaler Momente

Der Zentraldetektor des KASCADE Experimentes ermöglicht Beobachtungen von Dichteverteilungen der Hauptkomponenten im Zentrum von EAS. Insbesondere wird die Myonkomponente durch großflächige ortsauflösende Vieldraht-Proportionalkammern (MWPC) gemessen, die unterhalb des Hadronkalorimeters (1000 g/cm^2 Fe) installiert sind. Mit Hilfe der Methode der multifraktalen Momente, angewandt auf simulierte Daten, die direkt mit Meßdaten der MWPC vergleichbar sind, kann gezeigt werden, daß unterschiedliche EAS Lateralverteilungen durch die Art des Primärteilchens bedingt sind. Erste Vergleiche mit gemessenen Daten der MWPC werden durchgeführt.

1 Introduction

The detailed structure of the lateral particle density distribution of an extensive air shower (EAS) carries valuable information on the shower development and the nature of the shower inducing cosmic ray primary. This is, in particular, true for the penetrating muon component, as it is not subject of relevant Coulomb scattering and further cascading, thus directly related to the details of the nuclear interactions in the EAS core. The essential effects originate from the height at which the parent particles (pions and kaons) decay and from the transverse momentum distribution of the parent pions (kaons). Therefore, though contributing only with approximately 10% to the total number of charged particles and photons (with energies above 300 MeV at sea level), the shape of the lateral muon distribution should provide some information on the longitudinal development of EAS, and as consequence some signatures for the mass of the primary - in addition to the total muon number N_μ, which is determined by the multiplicity of secondary production in high-energy hadronic interactions.

The central detector of the KASCADE (KArlsruhe Shower Core and Array DEtector) experiment [1] is equipped with a muon detection facility [2] consisting of 32 position-sensitive multiwire proportional chambers (MWPC) with a rather good spatial resolution ($\approx 5\ mm$) and a good coverage of the area in the basement, i.e. below the iron-sampling calorimeter ($\approx 1000\ g/cm^2$). They are triggered with fast scintillation detector devices, presently by an array ('Top-Cluster') of 16 detectors on top of the central detector. The task of the MWPC arrangement in context of the KASCADE experiment is the determination of the lateral muon distribution and of the local muon number in the shower core.
However, there are various difficulties of the present configuration in cases of high-energy particles densities. Due to the relative large size of the single MWPC there are reconstruction ambiguities for larger muon multiplicities per chamber. Secondaries, i.e. δ-electrons, electrons from muon induced showers, and the 'punch-through' of high-energy hadrons obscure the identification of the muons, in addition.

In the present work the features of the lateral particle distributions, virtually of the muons, in the shower core are analyzed, based on simulated air shower data in the PeV region, including the distortion, when crossing the KASCADE central detector setup and with the response of the MWPC detector facility.
The quantification of structural differences of the distribution resulting from different primaries uses the method of a multifractal moment analysis, which has been shown to be useful in identifying structures of various distributions.
This method has been recently introduced for an analysis of the lateral distribution of the e/γ component for observed air showers [3, 4], revealing discriminating features for different types of primaries.

1

We finally demonstrate our procedures and the method of analysis by considering real data, measured with the actual MWPC arrangement of the KASCADE central detector.

2 Simulation Studies

2.1 Simulation of Extensive Air Showers

As first step a set of realistic shower data for the observation level of KASCADE (110 m a.s.l.) is generated by Monte-Carlo simulations of the shower development in the atmosphere, using the program CORSIKA [5].

The CORSIKA program has been specifically developed to perform simulations for the KASCADE experiment. It uses a Monte-Carlo generator based on the Dual-Parton Model [6, 7]. This model describes the hadronic interactions of protons at high energies in agreement with measured collider data. The model is extended to the interaction of complex primary nuclei by calculating the fraction of interacting nucleons in target and projectile, invoking the superposition hypothesis. Diffractive reactions are included. For the comprehensive simulation of the electromagnetic component the EGS4 code [10] is included. But in our calculations the faster NKG approximation is used.
A recent version of CORSIKA (Version 4.068) is modified by the GEISHA program [8] included for describing the hadronic interaction below $E_{cm} = 12$ GeV and by the VENUS program [9] to handle very high-energy interactions.

The energy range of the simulated showers extends from $1 \cdot 10^{15}$ eV to $3.16 \cdot 10^{15}$ eV. Lower primary energies do not induce the necessary hit density below the shielding of the central detector for an useful analysis of multifractal moments.

primary particle	primary energy [eV]	shower size $logN_e$	shower age s
proton	$1.00 \cdot 10^{15}$	5.05 ± 0.20	1.30 ± 0.06
proton	$1.40 \cdot 10^{15}$	5.26 ± 0.20	1.30 ± 0.05
proton	$1.78 \cdot 10^{15}$	5.39 ± 0.23	1.29 ± 0.06
iron	$1.78 \cdot 10^{15}$	5.04 ± 0.08	1.32 ± 0.02
iron	$2.60 \cdot 10^{15}$	5.20 ± 0.08	1.32 ± 0.02
iron	$3.16 \cdot 10^{15}$	5.33 ± 0.07	1.32 ± 0.02

Table 1: Simulated shower groups.
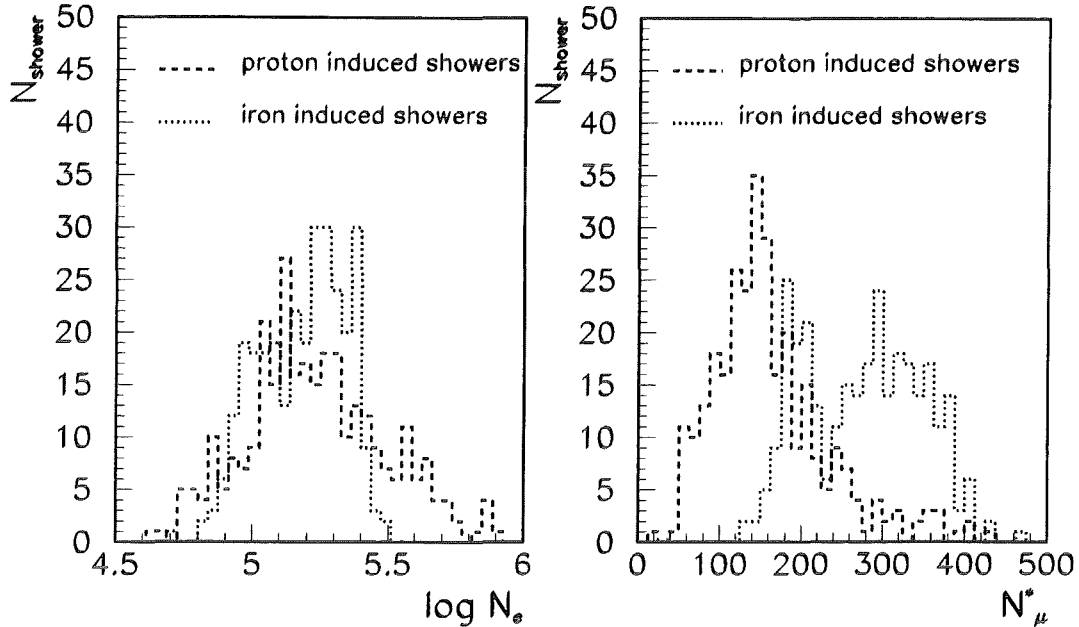
Figure 1: Shower size N_e and number of muons N_μ^* $(E_\mu > 2\ GeV$ within a distance to the core of 8 m) of 600 showers simulated by CORSIKA.

The flux of showers with higher energy is to low for a survey in comparison with KASCADE data. The shower size N_e (measurable by the KASCADE array) is an important parameter classifying the shower events used in the analysis of MWPC data. In order to provide the same N_e range for proton induced and iron induced showers the primary energy of the latter one has to be increased. Due long computing times, only relatively small samples of showers are generated in six different groups (Tab. 1). We consider air showers with vertical incidence and the core positioned in the center of the central detector.

All muons and hadrons with an energy threshold of 2 GeV and with a maximal distance to the shower center of 8 m are considered in the further discussion. The cuts approximately correspond to the sensitive area of the multiwire proportional chambers and the shielding of the central detector at KASCADE.
Fig. 1 displays the distributions of the shower size and number of muons N_μ^* $(E_\mu > 2\ GeV,\ R_\mu < 8\ m)$ of the used simulated air showers as calculated by the CORSIKA code. The muon number N_μ^* is a measurable quantity. Fig. 1 indicates that the muon number N_μ^* provides a signature for mass separation.

3
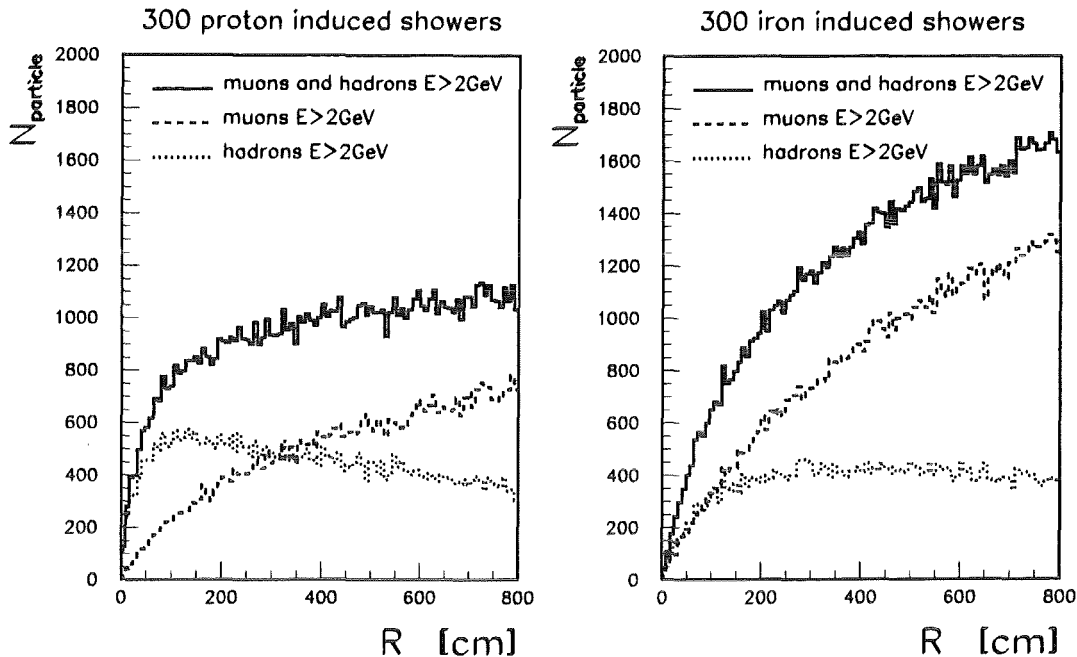
Figure 2: Lateral distributions of muons and hadrons near the core of showers induced by proton and iron primaries, calculated by the CORSIKA program.

Multifractal moments examine density structures of the distribution of muons and hadrons. Fig. 2 gives evidence for differences of the central part of the lateral distributions of showers initiated by protons and by iron nuclei, respectively. But they are hardly observable in experiment.

2.2 Simulation of the KASCADE Central Detector

The general layout of KASCADE includes a detector array with a total area of $200 \cdot 200 \ m^2$ and a central detector consisting of a hadron calorimeter of $20 \cdot 16 \ m^2$ and nearly $300 \ m^2$ multiwire proportional chambers in the basement below for muon detection.

The array consists of 252 detector stations, organized in 16 subarrays, each forming a quadratic grid of $13 \cdot 13 \ m^2$ for sampling the electromagnetic and muonic components with their lateral distributions. It provides the basic information about the shower size N_e, the location of the core, arrival direction, and the arrival time of the shower front.

4

KASCADE Central Detector   20m x 16m x 4m
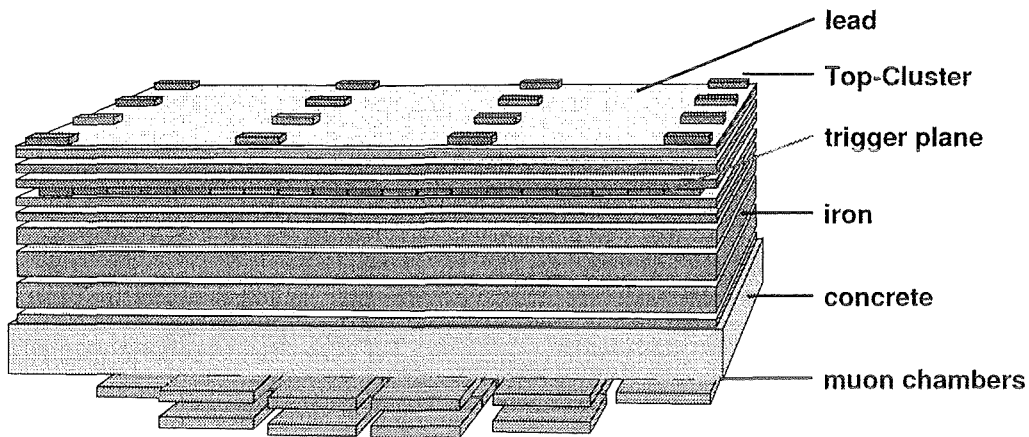
Figure 3: Schematic view of the central detector of KASCADE.

The central detector has various parts (Fig. 3):

- a sampling calorimeter (20 · 16 m^2 with 3800 t iron as passive layers) for measuring the energy spectrum and the lateral distribution of hadrons in the shower core;

- one active layer of the calorimeter setup is a trigger and timing facility, enabling arrival time measurements;

- on top of the central calorimeter there is an e/γ mini array: the Top-Cluster, coupled to the full array and for studying the density in the core;

- multiwire proportional chambers installed in the basement for measurements of muons of an energy threshold of 2 GeV.

The whole detector field is covered with detectors to 2.5% for muons, 2.0% for electrons-photons and 0.6% for hadrons. The expected rates for showers having the core inside the central detector are 50 per hour for $E_0 > 10^{14}$ eV and 4 per day for $E_0 > 10^{16}$ eV.

With the GEANT code [11] included in the simulation program the distribution of measurable hits in the multiwire proportional chambers below the iron shielding of the calorimeter is studied. All muons and hadrons at energies higher

5
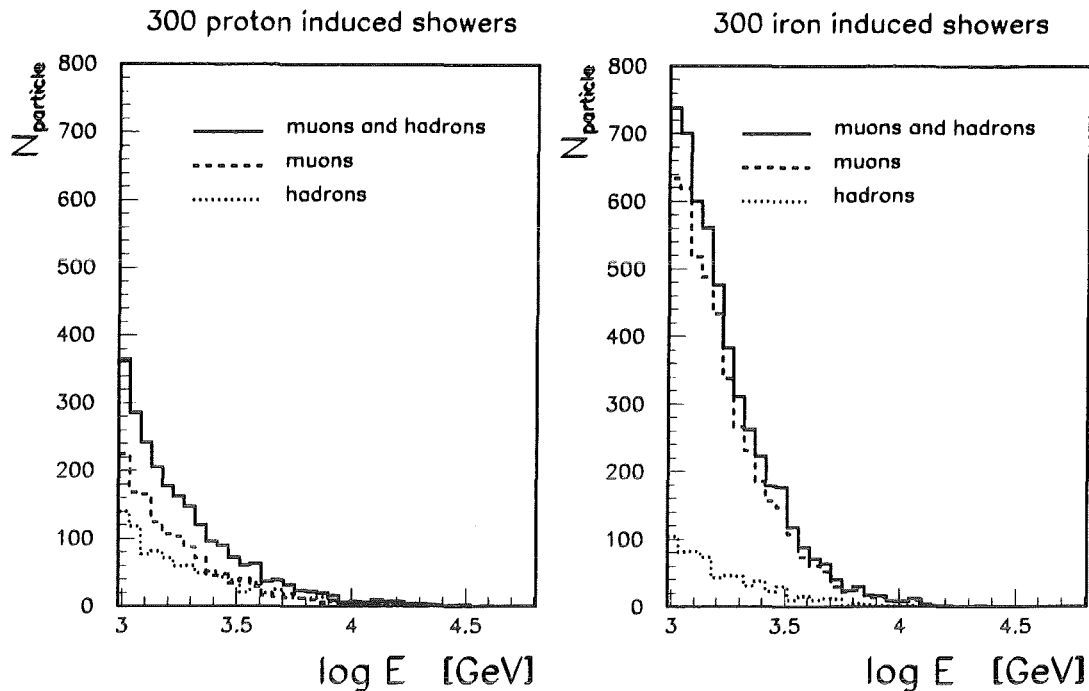
Figure 4: Spectra of high-energy particles ($E > 1$ TeV) from proton and iron induced showers with equal size ($logN_e$ = 4.5 − 6.0), simulated by CORSIKA.

than 2 GeV and hitting the central detector are tracked through all shielding materials. The simulation of the 5.0 cm lead absorber, all layers of iron, and the ceiling of concrete at the basement are handled correctly in material and geometrical structures. The scintillation detectors and the sensitive calorimeter layers are neglected in this detector simulation. All relevant physical interactions of particles with matter are taken into account and each produced secondary particle is tracked through the calorimeter.

Before starting a detailed simulation of the response of the MWPC setup we examine all particles produced in the shower and in the material of the shielding. So we replace the real chambers by a 16 mm thick active gas layer. This gas layer is circular and has a size of $R = 8$ m in radius. The detection threshold equals the real one, but the active area is assumed as 100 % with an infinite spatial resolution. This procedure facilitates the comparison of raw shower data of the CORSIKA simulation with detectable data after the GEANT simulation of the different absorption layers. In this fictive gas layer there are either single particles or clusters of many particles detectable.
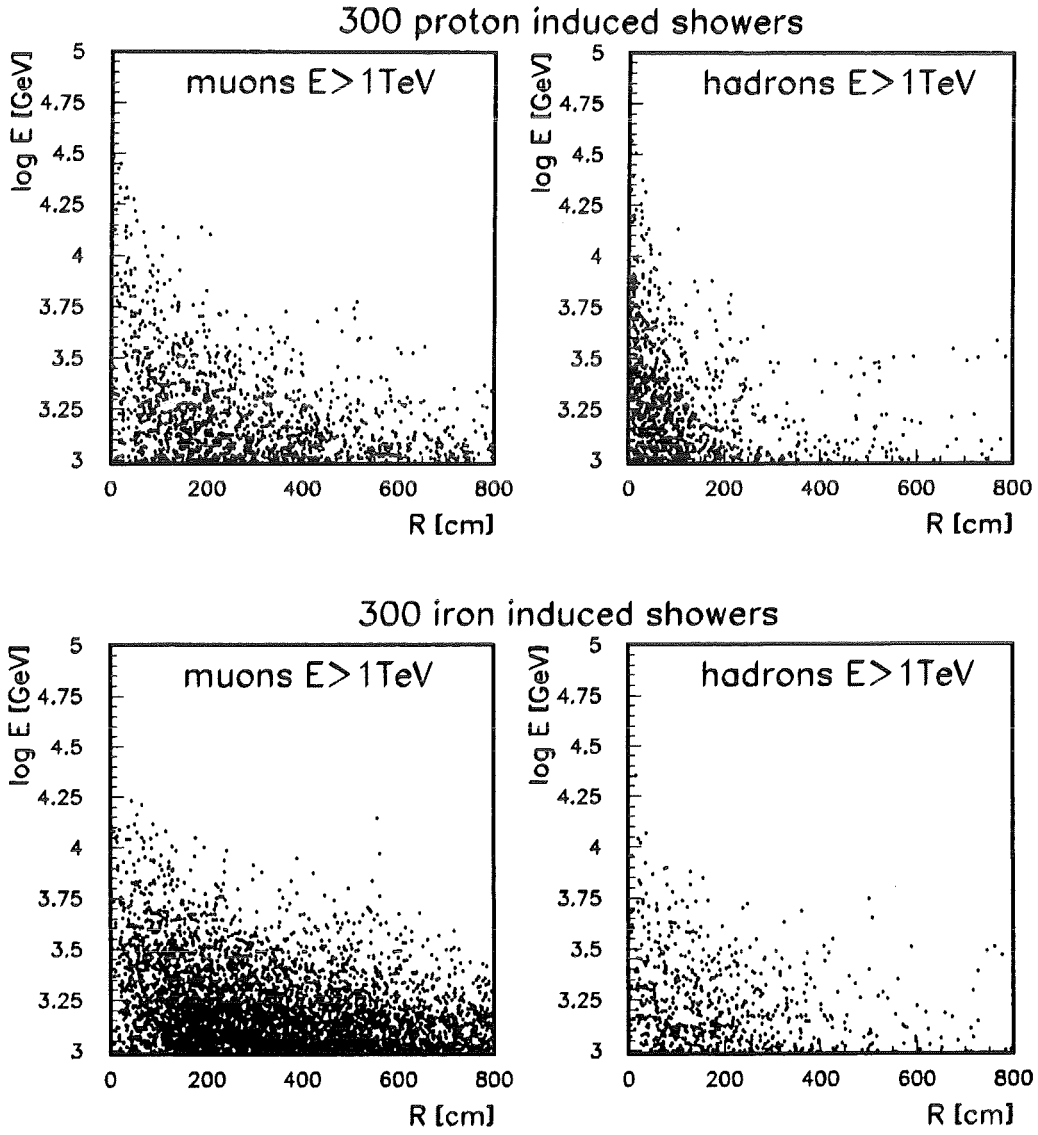
Figure 5: Radius-energy-correlation of high-energy particles ($E >$ 1 TeV) from proton and iron induced showers with equal size ($log N_e = 4.5 - 6.0$), simulated by CORSIKA.

Hits and clusters of different sizes have various origins:

- Muons, passing the shielding without any interaction.

- δ-electrons, created at the lower end of the shielding (seen mostly with the muon as a pair of two neighbored hits).

- Small clusters produced by electromagnetic showers induced by pair production of the muons or by conversion of photons from muon bremsstrahlung or by cascading of δ-electrons.

- Clusters of electromagnetic particles from surviving secondaries of hadronic showers stopped at the calorimeter (neutrons).

- Large clusters from secondaries of hadrons with energies larger than being absorbed by the calorimeter ($E_h > 10\ TeV$).

- There are rare large clusters produced by nuclear interaction of muons with matter. With increasing muon energy the frequency of such interactions is increasing.

In section 3 it will be shown, that multifractal moments are extremely sensitive to the abundance, distribution and size of such clusters. Muons and hadrons with energies above 1 TeV promote the appearance of particle clusters. Thus the abundance (Fig. 4) and the distribution (Fig. 5) of shower particles with $E > 1\ TeV$ are expected to provide signatures for the mass of the primary. Fig. 4 shows the discrimination between proton induced showers and iron induced showers, first in the total number of high energy particles (due to the higher primary energy at iron showers at same shower size) and secondly through the muon-hadron number ratio. A further difference is seen in the lateral distributions of shower particles with energies $> 1\ TeV$ (Fig. 5): proton induced showers concentrate a larger amount of energy in the innermost part ($R < 2\ m$) of the shower than iron induced showers do.

2.3 Response of the KASCADE Multiwire Proportional Chambers

In order to include the response of the MWPC, at the position of the fictitious gas detector, (see sect. 2.2), each particle is tracked in the system of the muon chambers. Fig. 6 shows the schematic view of the 32 multiwire proportional chambers at the basement. There are 16 stacks of two chambers each. In the basement there are six columns of concrete. The stacks are placed around this columns in order to get an optimal coverage of sensitive area in the center of the basement. The detailed simulation of this setup using the GEANT code is

Muon Chambers at the Central Detector
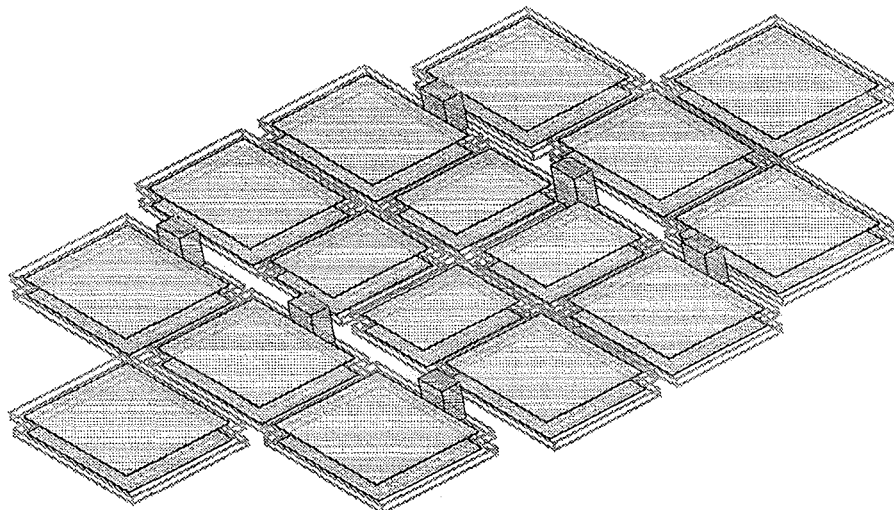
sensitive area: 2 x 122 m^2

area of basement: 20 x 16 m^2

Figure 6: Schematic view of the 32 KASCADE multiwire proportional chambers.

described in [12]. The detected particles in the detector system are expressed in numbers of wires and stripes and stored in the same way as real measured data. The simulated multiplicity of wires and stripes for one hit represents the real behavior of the chamber response [13].

An algorithm [14] reconstructs in a first step hits (the position where particles penetrate the chambers) for every individual chamber and, in a second step, position and angles of muons and the position of clusters by combining both chambers of each stack [15]. A cluster is defined as an accumulation of hits in a limited area (50 · 50 cm^2 in both chambers of a stack). The MWPC cover 60% of the circular area used for the analysis of multifractal moments.

The number of muons N'_μ in the central detector at each shower is well determined with the used algorithm. The recognition of clusters and the discrimination of δ-electrons, secondary particles and ambiguities in the hit reconstruction are working as well. But the statistics of the muon lateral distribution in individual

9

proton induced shower
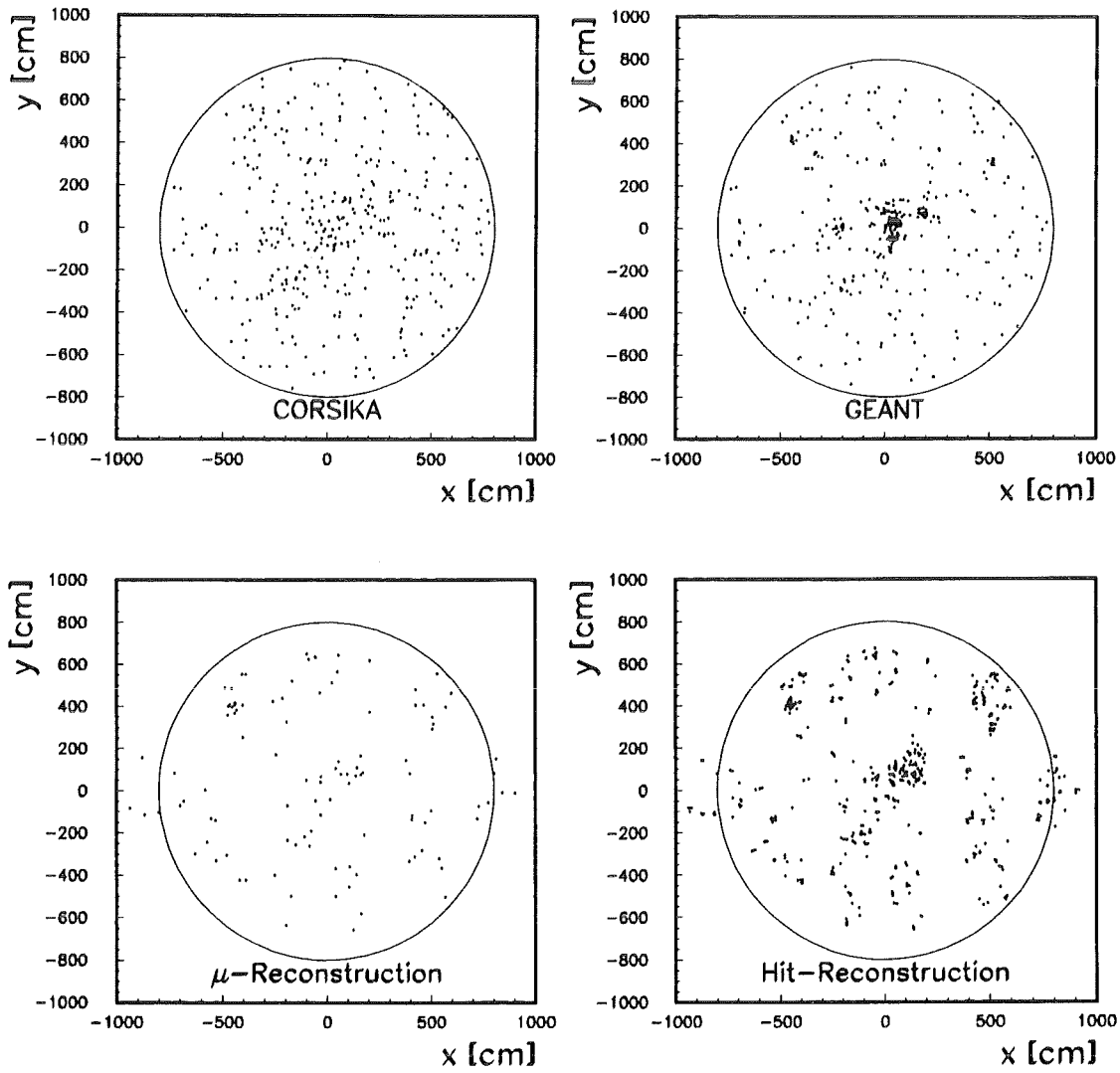
Figure 7: An example of the two-dimensional density distributions observed in the different steps of the simulation of a proton induced shower. The circles display the used area for the calculation of multifractal moments.

10

iron induced shower
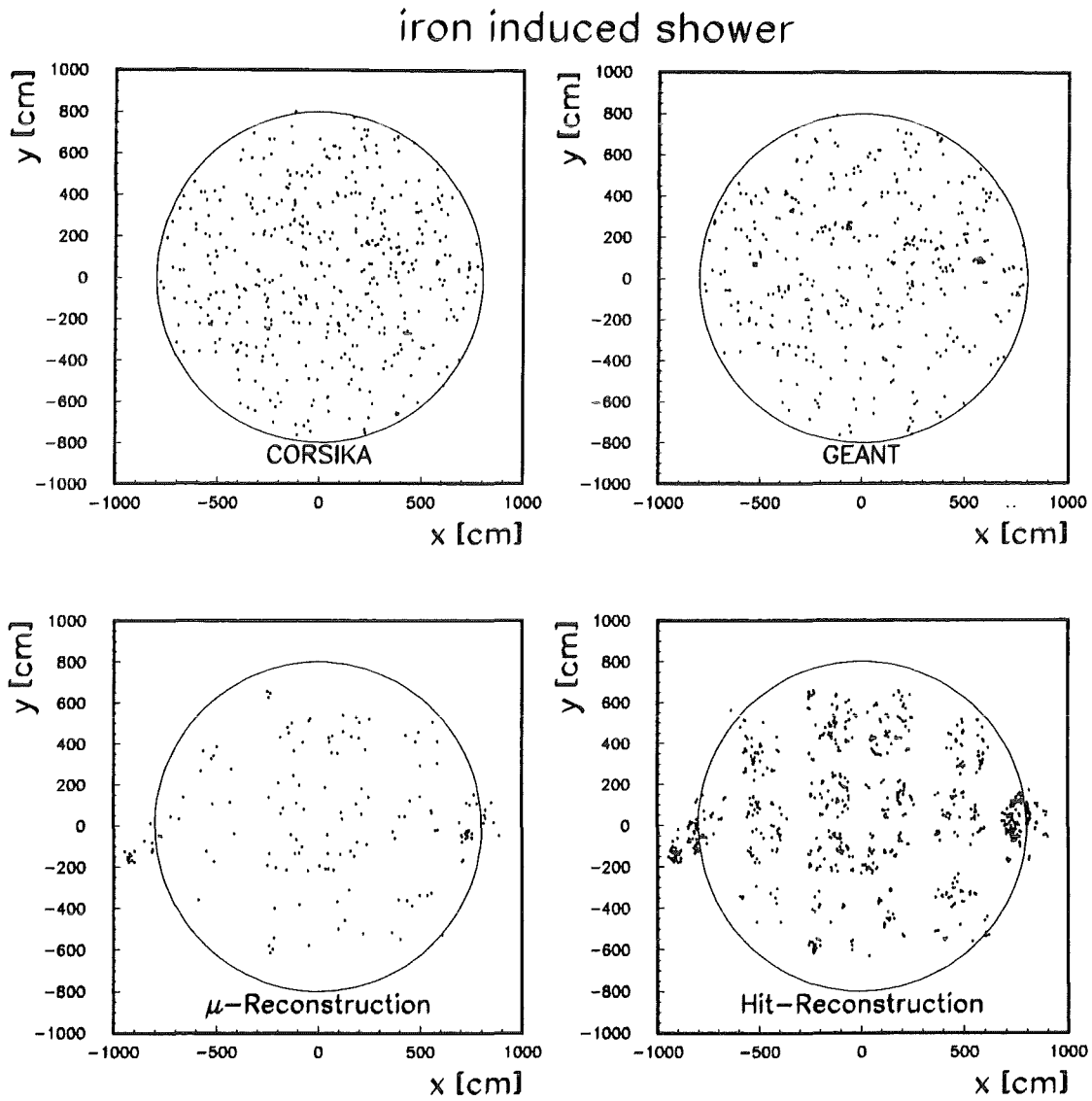
Figure 8: An example of the two-dimensional density distributions observed in the different steps of the simulation of an iron induced shower. The circles display the used area for the calculation of multifractal moments.

showers are too small, and thus there are rather large fluctuations for each individual shower group.

In order to prepare the analysis through multifractal moments of realistic data, in a next step all reconstructed hits in both chamber layers are added to the found muons and clusters.
In this form of presentation of measured data we have a double weight of the muons (once as reconstructed muon, once as hit) and a single weight of all secondaries. The secondaries are complicating the reconstruction of muon numbers. Nevertheless, there is an information of the shower development inside the density structures with regard to this secondaries.

Figs. 7 and 8 display the obtained density distributions of a proton and a iron induced shower, respectively, in the core ($R < 8\ m$) for all four steps of the simulation study:

1. CORSIKA-step: all muons and hadrons above 2 GeV obtained by pure shower simulation with CORSIKA.

2. GEANT-step: all particles from step 1 which penetrate the shielding, and all secondaries produced in the shielding.

3. μ-reconstruction: detailed reconstruction of muons and clusters from the data seen by chambers.

4. Hit-reconstruction: reconstruction of muons and clusters and counting of all reconstructed hits of every chamber.

The shown proton (iron) shower has a primary energy of $1.78 \cdot 10^{15}\ eV$ ($3.16 \cdot 10^{15}\ eV$) and a shower size of $logN_e = 5.33$ ($logN_e = 5.30$). It is obvious that, first of all, the structure in the lateral density distribution is the result of clusters originating from high-energy particles in the central detector. Differences of the lateral particle distributions are visible in the reconstruction, if all information for reconstruction is taken into account.

3 The Analysis of Multifractal Moments

The analysis of multifractal moments is a mathematical method to reveal and to quantify structures of multidimensional density distributions [16, 17]. The multifractal analysis has been successfully applied in the investigations of various properties of different systems: for particle clustering in the high-energy interactions [18, 19] as well as for the fractal structure of the Universe [20]. Also in cosmic ray physics multifractal studies have been introduced. With data from

the Kiel air shower experiment [4] done in the late seventies, differences in density structures of electrons of differently induced air showers have been revealed [3, 21, 22].

For a brief reminder, Fig. 9 displays two examples of hit distributions obtained by shower simulations (CORSIKA) and simulations of the KASCADE central detector (see chapt. 2).
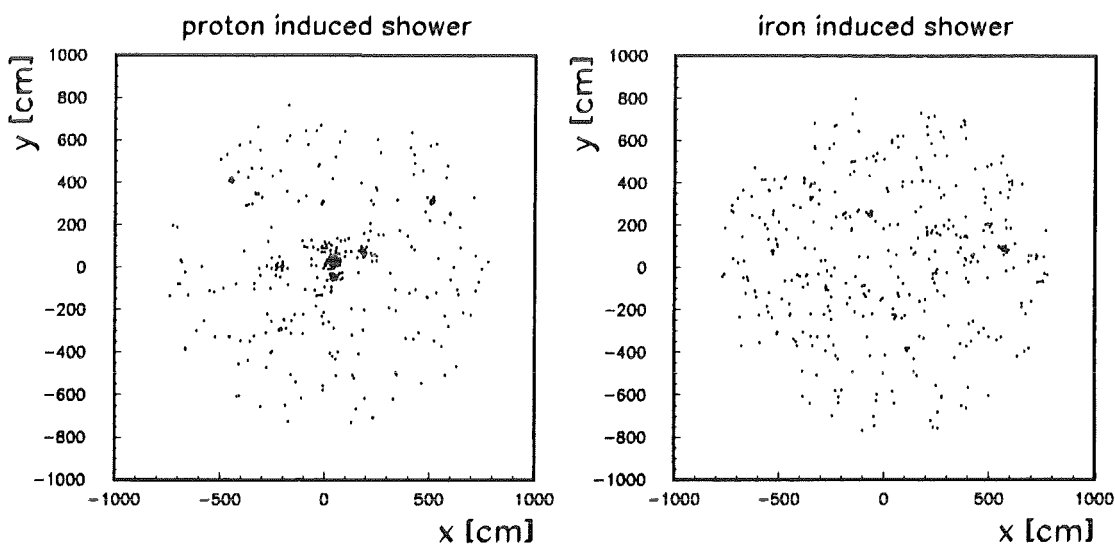
Figure 9: Two examples of two-dimensional hit distributions in the shower core obtained by EAS simulations including the detector response.

For the calculation of the multifractal moments we divide the area of the two-dimensional density distribution in M = 2, 4, 8, and 16 circular, equally sized areas and determine the number of hits in each ring.

The multifractal moments G_q are defined by:

$$G_q = \sum_{j=1}^{M} (k_j/N)^q$$

where M is the number of used circular areas, k_j the number of hits per ring, N the total number of hits and q is a real number. The moments are calculated for $-6 \leq q \leq 6$. The summation is carried out over non-empty bins only.

13
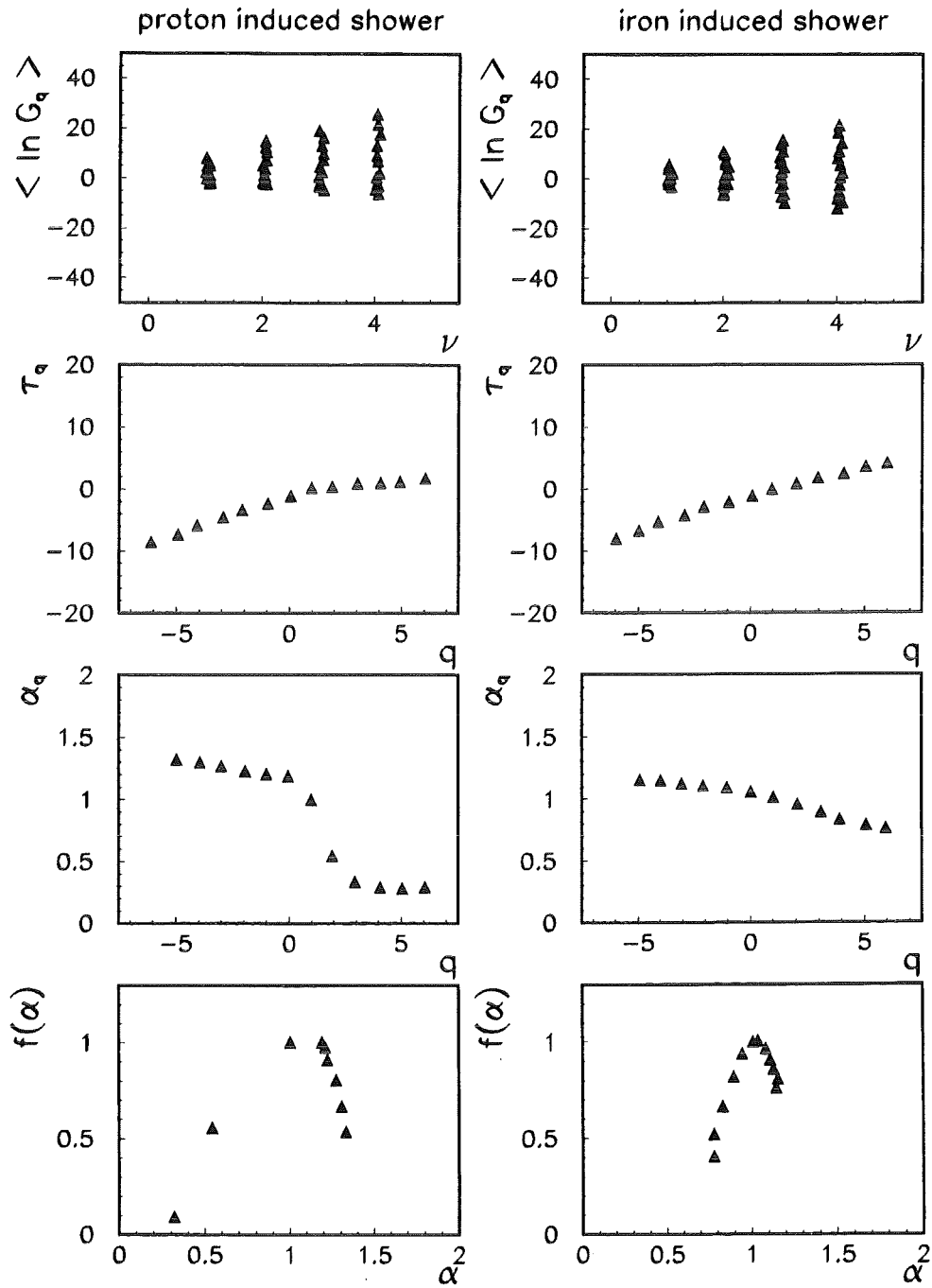
Figure 10: Various steps of the analysis of hit distributions by multifractal moments. The multifractal dimensions of the proton shower are $D_6 = 0.35$ and $D_{-6} = 1.22$. The iron shower has the values $D_6 = 0.84$ and $D_{-6} = 1.09$.

If the detected particles exhibit self-similar behavior [20], the moments G_q show a power-law relation

$$G_q \sim \delta^{\tau_q}.$$

The exponent τ_q is determined from G_q. The values of the logarithm of the multifractal moments are calculated for different numbers of circular areas ($M = 2^\nu$) and are shown for the two examples in Fig. 10. For determining the slope via the formula

$$\tau_q = -\frac{1}{ln2} \cdot \frac{d(lnG_q)}{d\nu}$$

the values between $\nu = 1$ and $\nu = 4$ have been used. The q-dependence of the exponent τ_q is also shown in Fig. 10.
A commonly used function

$$f(\alpha) = q \cdot \alpha_q - \tau_q$$

contains all information about differences of the structure of density distributions [20]. This function $f(\alpha)$ is calculated by a Legendre transformation with α_q being the Lipschitz-Hölder exponent

$$\alpha_q = \frac{d\tau_q}{dq}.$$

In the lower part of Fig. 10 the functions $\alpha_q(q)$ and $f(\alpha)$ are shown.
The minimum value of α is associated with large q-values and characterizes the strongest singularity in the system. It is related to the proportion of the largest hit cluster to the overall density. Related to negative q-values there is a maximum value α_{max}, which emphasizes the regions with lowest hit density in the system. Both parameters are sensitive to the mass of the primary nucleus. There is a direct correlation between the parameters α_{min} and α_{max}, respectively and the slope of the function $f(\alpha)$ at different α-values. This correlation is described by the *generalized multifractal dimensions*

$$D_q = \frac{\tau_q}{q - 1}$$

of the corresponding q-values. Consequently the further analysis of the data considers the multifractal dimensions D_6 and D_{-6} as characteristic parameters.

4 Results of the Analysis

4.1 Simulation Results

In Fig. 11 the multifractal dimensions D_6 and D_{-6} are displayed in a two-dimensional scatter plot. In case of the MWPC response reconstruction (steps 3 and 4) we correct the number of counted hits in different rings for the sensitive area.

For a more compact illustration of the separation quality of the D_6 - D_{-6} distributions, we introduce a new parameter P, a linear combination of D_6 and D_{-6}, arising from a coordinate rotation, with the abscissa defined by the points ($D_6 = 0.5$, $D_{-6} = 1.0$) and ($D_6 = 1.0$, $D_{-6} = 1.5$). In Fig. 12 the distribution of the parameter P is plotted, indicating the quality of the mass separation. It is also shown that the reconstructed lateral muon distributions alone are less indicative. However the summed muon numbers in the first 8 m around the shower center (the 'theoretical' N_μ^* in case of CORSIKA and GEANT-simulations and the 'observed' N_μ' in case of the MWPC data reconstruction) prove to be a powerful separation quantity. The reconstructed N_μ' of the MWPC have an uncertainty of ca. 10 %. Fig. 13 shows the three-dimensional distribution of the shower events in the D_6, D_{-6}, $N_\mu^*(N_\mu')$ parameter space.

For showers with similar shower sizes ($logN_e = 5.2 - 5.7$) and similar muon numbers ($200 \leq N_\mu^* \leq 300$) it is seen that the multifractal dimensions and the muon numbers are not correlated (Fig. 14).

4.2 Remarks on Extensions of the Analysis

For a more detailed understanding of the method and of the sensitivity of multifractal dimensions some dependencies of the method are studied. The Figs. 15, 16, 17 show final results of the hit-reconstruction.

4.2.1 Alternatives to circular areas

Instead of 16 rings around the center one single circular ring area has been subdivided in 16 azimuthal sectors [21]. In this case the multifractals are sensitive to fluctuations and the radial anisotropy of structures in the densities. This procedure is useful for the examination of electron densities of high energy air showers. Fig. 15 displays an attempt to use such sectoral structures for the simulated showers. The used ring covers the area between $R = 2$ m and $R = 8$ m and is divided in equally-sized sectors. The most powerful feature for mass separation by the data of multiwire proportional chambers is the lateral distribution of the particles with highest energies in the shower (Fig. 5). This is confirmed by the missing separation of iron to proton induced showers in Fig. 15.

16
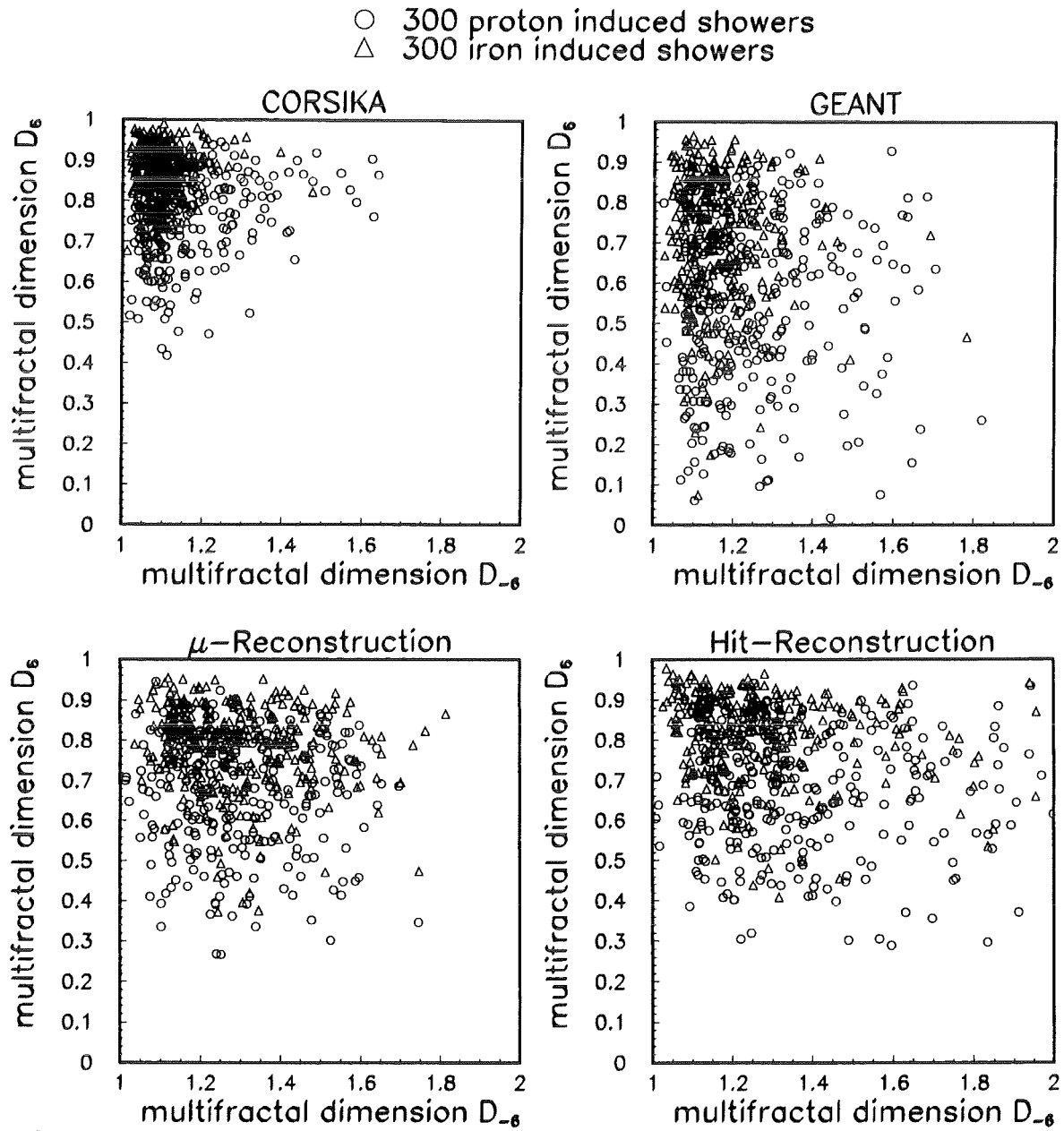
Figure 11: Distributions of the multifractal dimensions D_6 - D_{-6} for all four steps of the simulation procedure.
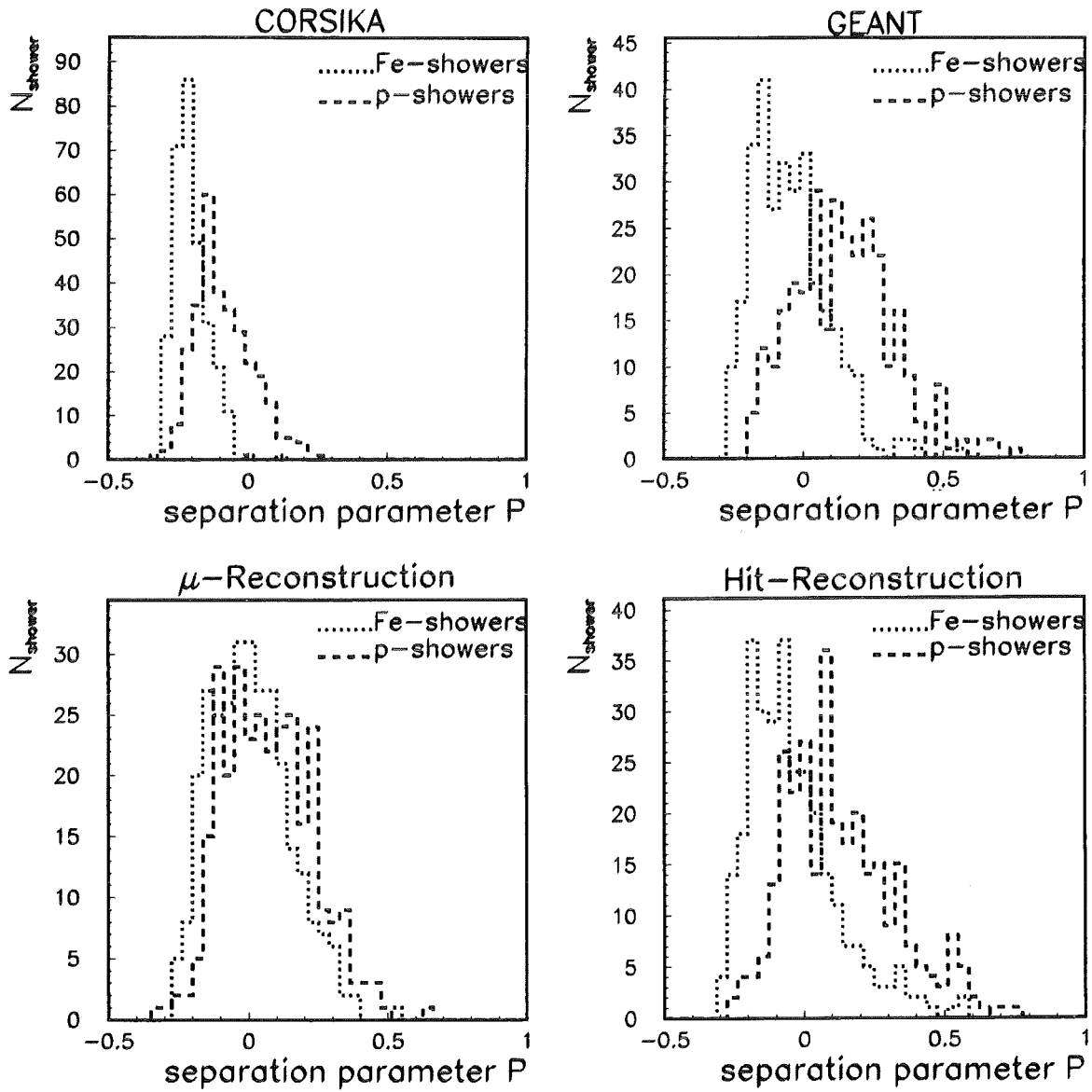
Figure 12: The distribution of the parameter P, defined as a linear combination of D_6 and D_{-6} by introducing an adequate, rotated coordinate system in the D_6 - D_{-6} plane (see text).

18
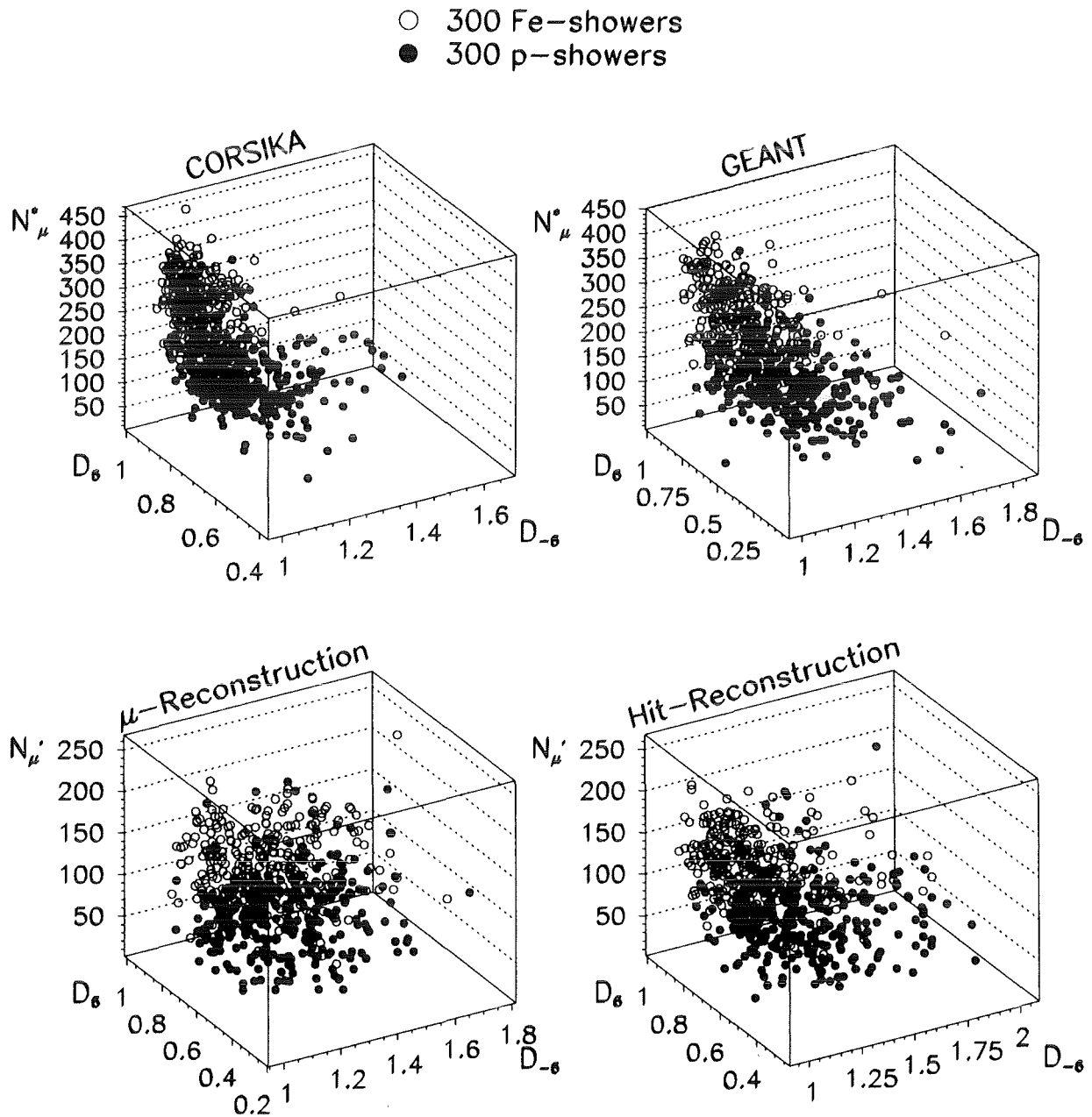
Figure 13: Three-dimensional distributions of parameters observable by the multiwire proportional chambers in all subsequent steps of the simulation procedure.

19
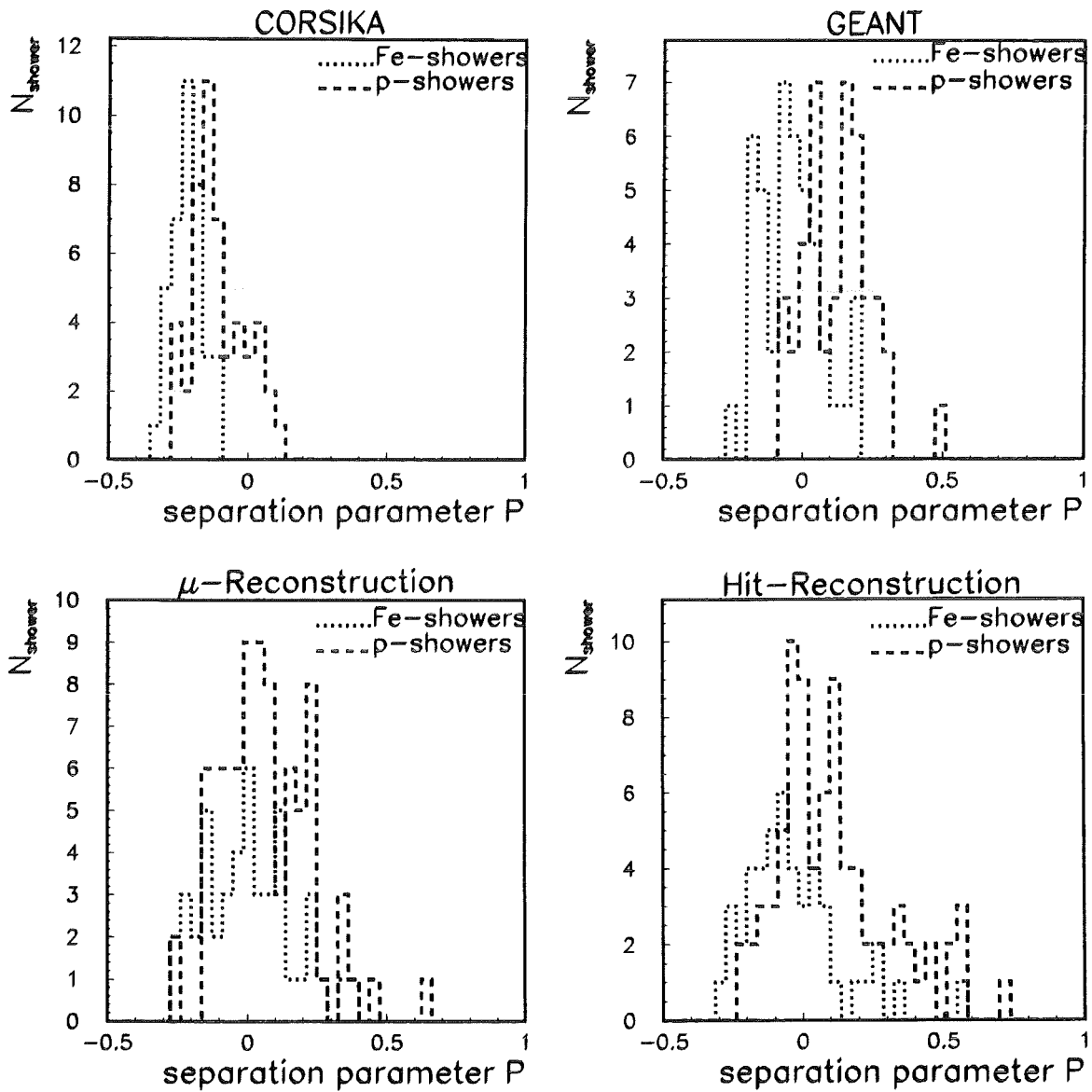
Figure 14: The distribution of the separation parameter P for showers of equal shower sizes and equal numbers of muons in all subsequent steps of the simulation procedure.
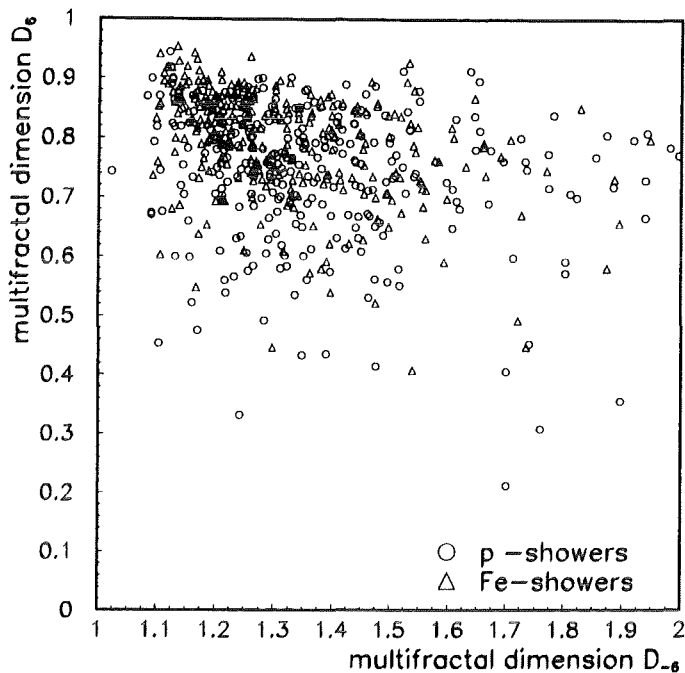
Figure 15: Distribution of the multifractal dimensions using a sectoral structure of the circular area instead of a ring structure.

4.2.2 Inclined showers

All statements resulting from the analysis of showers of vertical incidence prove to be generally valid for inclined showers. Fig. 16 shows the result of the calculation of multifractal dimensions of 100 proton and iron induced showers each hitting the central detector with the zenith angle of 20^0. The used showers have fixed primary energies of $1.78 \cdot 10^{15}$ eV for the proton induced showers and $3.16 \cdot 10^{15}$ eV for the iron induced ones. These energy values are at the upper end of the spectrum which is used for the vertical showers. The multifractal dimensions prove to be slightly more sensitive due to the higher probability of cluster formation. The separation (Fig. 16) appears to be clearer for inclined showers than for vertical showers.

4.2.3 Estimation of the location of shower core

In all used simulations the position of the shower core is assumed to be exactly at the center of the central detector. The determination of the location of the shower core will be done with the array of KASCADE and for showers falling in the cen-
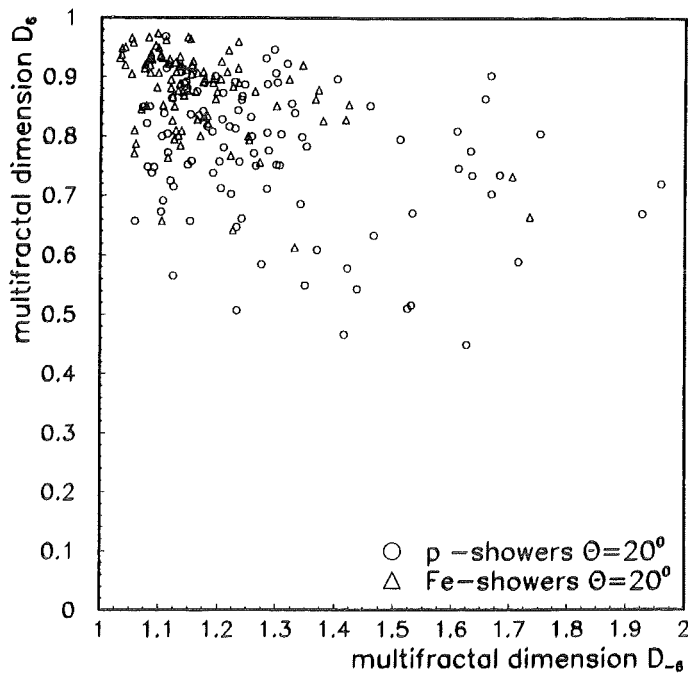
Figure 16: Distribution of the multifractal dimensions of inclined showers.

tral detector with an additional information by the hadron density observed in the calorimeter. Calculations with slightly shifted shower centers show that an uncertainty in the estimation of the shower core position of $1 - 2$ m does not change essentially the results for mass separation with multifractal dimensions. At primary shower energies $E > 1 \cdot 10^{15}$ eV such an accuracy in core location is expected to be reached with the KASCADE array [23].

4.2.4 Effects of the primary energy spectrum

The steeply decreasing primary energy spectrum will cause problems of the estimation of the primary mass composition. Showers with similar sizes N_e, but from different masses of the primaries are significantly different in the primary energy. Thus the abundance of differently induced showers is different in measured N_e groups. In a more detailed analysis this can be remedied by the 'a-priori' knowledge on the primary energy spectrum.

4.3 Comparison with measured KASCADE Data

The system of the multiwire proportional chambers with 28 of 32 chambers installed is in operation in a stand-alone mode since end of 1994. For triggering with the electromagnetic component of extensive air showers the scintillation detectors of the array on top of the central detector (Fig. 3) is used. The trigger condition is a coincidence of four detectors at the corners of the Top-Cluster. From the raw data the number and distributions of muons, number and distributions of particle clusters, the multifractal dimensions, and the direction of the shower are deduced by a detailed reconstruction procedure [15].
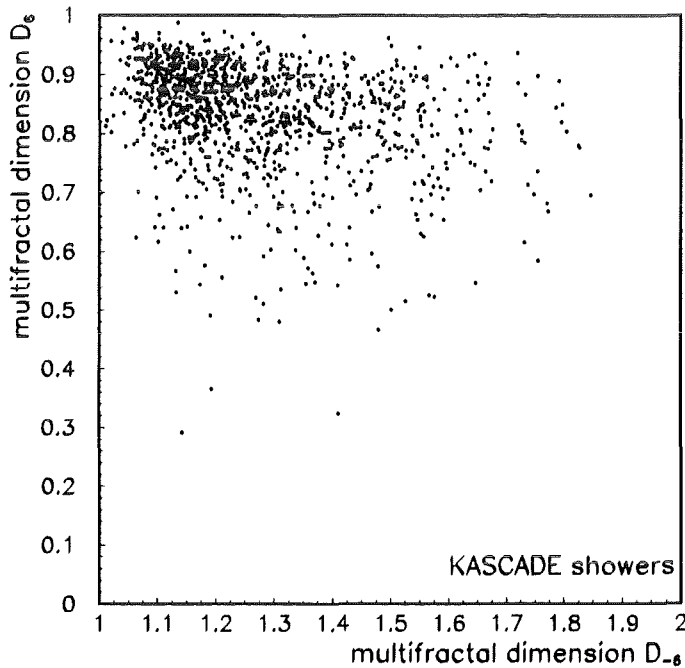
Figure 17: Distribution of the multifractal dimensions of shower data measured with the KASCADE central detector facilities.

The stand-alone system of the muon chambers is used for hard- and software tests of the setup. Currently the location of the shower core and the shower size N_e are important missing information for the analysis of measured showers by multifractal moments. Nevertheless, we could select 1161 from about 180000 registered showers by two simple cuts, requiring the reconstructed muon number

23

N'_μ with values between 50 and 150 and the center of gravity of the muon pattern positioned in a distance $< 70\ cm$ from the center of the central detector. Thus we approach the case of simulated showers. At least 75% of the simulated showers are within these cuts.

We conclude from this first analysis of measured data the feasibility of a useful analysis in terms of multifractal moments for KASCADE. It additionally confirms the correct reproduction of the KASCADE experiment by the detailed detector simulations. The distributions of the multifractal dimensions (Fig. 17) show this impressively. More definite conclusions on the mass composition, however, are presently not possible due to the uncertainty in the location of the shower core.

5 Concluding Remarks

The present study explores the potential of a multifractal moments analysis of high-energy air showers ($E > 10^{15}\ eV$) as a source of information for mass discrimination of the primaries. From EAS simulations with the CORSIKA code and subsequent detailed detector simulation of the MWPC facility of the KASCADE experiment, the MWPC arrangement (with large sensitive area and good spatial resolution) is shown to provide data useful for an informative multifractal moments analysis, thus establishing a new tool for studying the mass composition of cosmic rays.

Through measurements of the hit distribution by the multiwire proportional chambers the multifractal dimensions facilitate a discrimination between light and heavy primary induced showers. The additional determination of the muon numbers ($E_\mu > 2\ GeV$), registered by the MWPC, enhances the separation power.
It is interesting to realize that the detector response does not obscure the essential physical features of the shower appearance. The actual setup pronounces the sensitivity to the multifractal dimensions, and the information carried by the lateral particle distributions of the muon and hadron components, remains conserved. We stress that throughout our study only really measurable observables are considered and compared with theoretical EAS parameters.

Due to the excessive computer times, necessary for the detector simulation, this study is based on relative small samples of simulated showers. This might affect our results through the fluctuations of the high-energy particle cascading through the calorimeter. However, we expect that an improved statistical accuracy would confirm the global conclusions.
Alternatively to the use of the separation parameter P a well-founded mathematical procedure of pattern recognition of the distributions would possibly lead to

a more reliable distinction of proton and iron induced showers. Advanced techniques based on Bayes decision rules [24] or with a neural network analysis, like the recently successful analysis [25] of muon arrival time distributions, may be used.

In a first experimental approach a comparison with data measured by the KASCADE-MWPC detectors shows a good agreement in the multifractal parameters of simulated and measured EAS. When in near future the shower size and the location of the shower core will be available parameters for the reconstruction and specification of the MWPC data, a more detailed analysis towards primary mass information appears to be rather promising. The information may enter in a coherent analysis of a series of various shower parameters like the N_e - N_μ correlation, the energy deposit of hadrons in the calorimeter, the arrival time distributions of muons [25] etc., as a relevant signature for the mass composition of cosmic rays.

References

[1] G. Schatz, Interdiscipl. Sci. Rev. **18** (1993) 306

[2] P. Doll et al., KfK-Report 4686, Kernforschungszentrum Karlsruhe (1990)

[3] J. Kempa, J. Phys. G: Nucl. Part. Phys. **20** (1994) 215

[4] E. R. Bagge, M. Samorski, and W. Stamm, Proc. 16th Int. Cosmic Ray Conf. **13** (1979) 260

[5] J. N. Capdeville et al., KfK-Report 4998, Kernforschungszentrum Karlsruhe (1992)

[6] J. N. Capdeville, J. Phys. G: Nucl. Part. Phys. **15** (1989) 909

[7] A. Capella and J. van Tran Thank, Phys. Lett. **B93** (1980) 146

[8] H. Fesefeldt, Report PITHA 85/02, RWTH Aachen (1985)

[9] K. Werner, Phys. Rep. **232** (1993) 87

[10] W. R. Nelson, H. Hiroyama, and D. W. O. Rogers, SLAC Report 265 (1985)

[11] GEANT: (Version 3.21) CERN Program Library Long Writeups W5013 (1993)

[12] A. Haungs, Internal Report (1994), Kernforschungszentrum Karlsruhe, unpublished

[13] J. Wentz, FZKA-Report 5500, Forschungszentrum Karlsruhe (1995)

[14] H. J. Mathes, KfK-Report 5173, Kernforschungszentrum Karlsruhe (1993)

[15] A. Haungs et al., Spring Meeting of the German Physical Society: Particle Physics, Karlsruhe, March, 13-16, 1995

[16] B. B. Mandelbrot, J. Fluid Mech. **62** (1974) 331

[17] G. Paladin and A. Vulpiani, Phys. Rep. **156** (1987) 147

[18] A. Bialas and R. Peschanski, Nucl. Phys. **B273** (1986) 703

[19] R. C. Hwa and J. Pan, Phys. Rev. **D45** (1992) 1476

[20] P. H. Coleman and L. Pietronero, Phys. Rep. **213** (1992) 311

[21] A. Dudarewicz et al., Proc. 8th Int. Sym. on Very High Energy Cosmic Ray Interactions, Tokyo, Japan, July, 24-30, 1994, p.616

[22] J. Wdowczyk, J. Kempa, and M. Samorski, Izv. Akad. Nauk, ser. fiz. T.58, **12** (1994) 58

[23] H. J. Mayer, KASCADE-Workshop Bad Liebenzell (1991), unpublished

[24] A. A. Chilingarian, Comp. Phys. Comm. **54** (1989) 381

[25] H. Rebel, G. Völker, M. Föller, and A. Chilingarian, J. Phys. G: Nucl. Part. Phys. **21** (1995) 451

Appendix

Lateral Distributions of the Electron Component in the Center of High-Energy EAS

In this appendix electron density distributions for high-energy EAS, simulated by the Monte-Carlo code CORSIKA (using the EGS4 option and displayed with logarithmically varying bin sizes of R) are displayed. They indicate differences of the electron component for showers induced by different mass primaries, but they are evidently subject of large fluctuations.
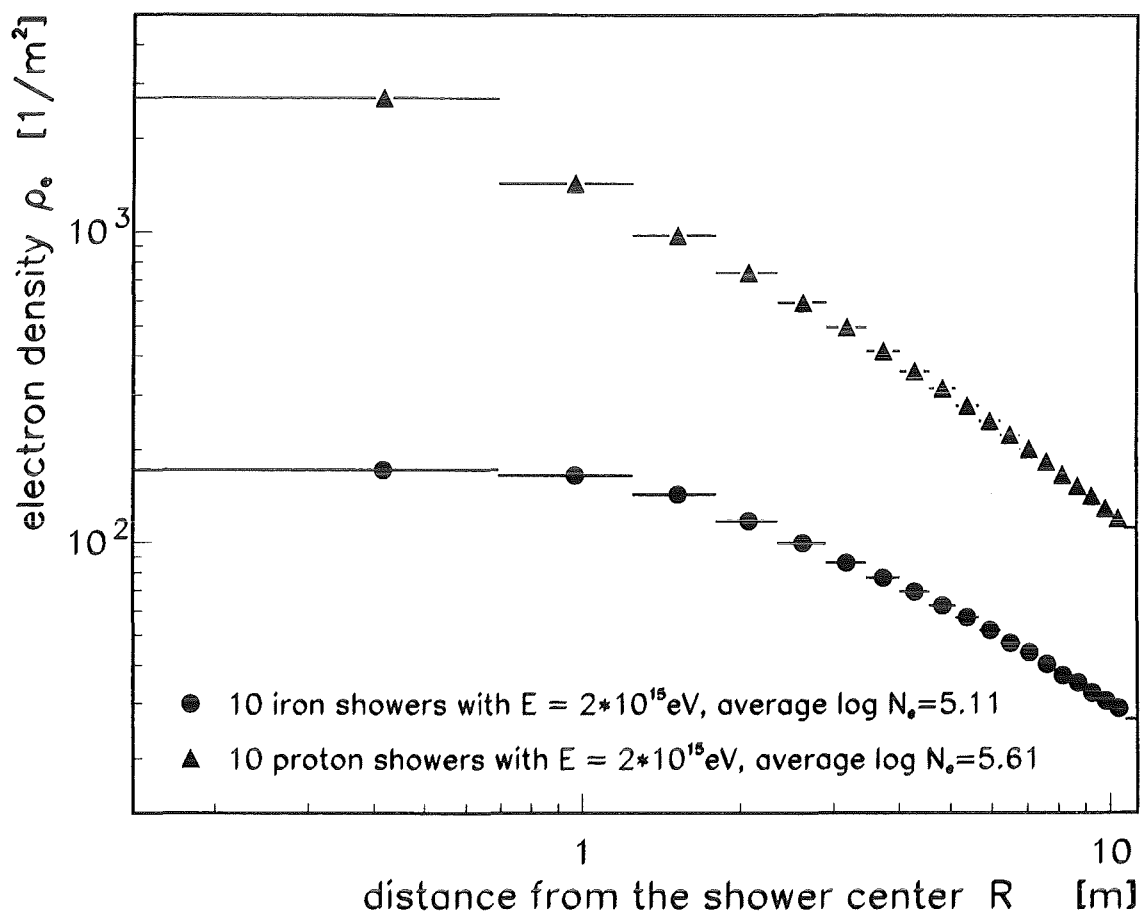
Figure A1: Averaged electron density distributions of iron and proton induced showers, claculated by CORSIKA (EGS4).
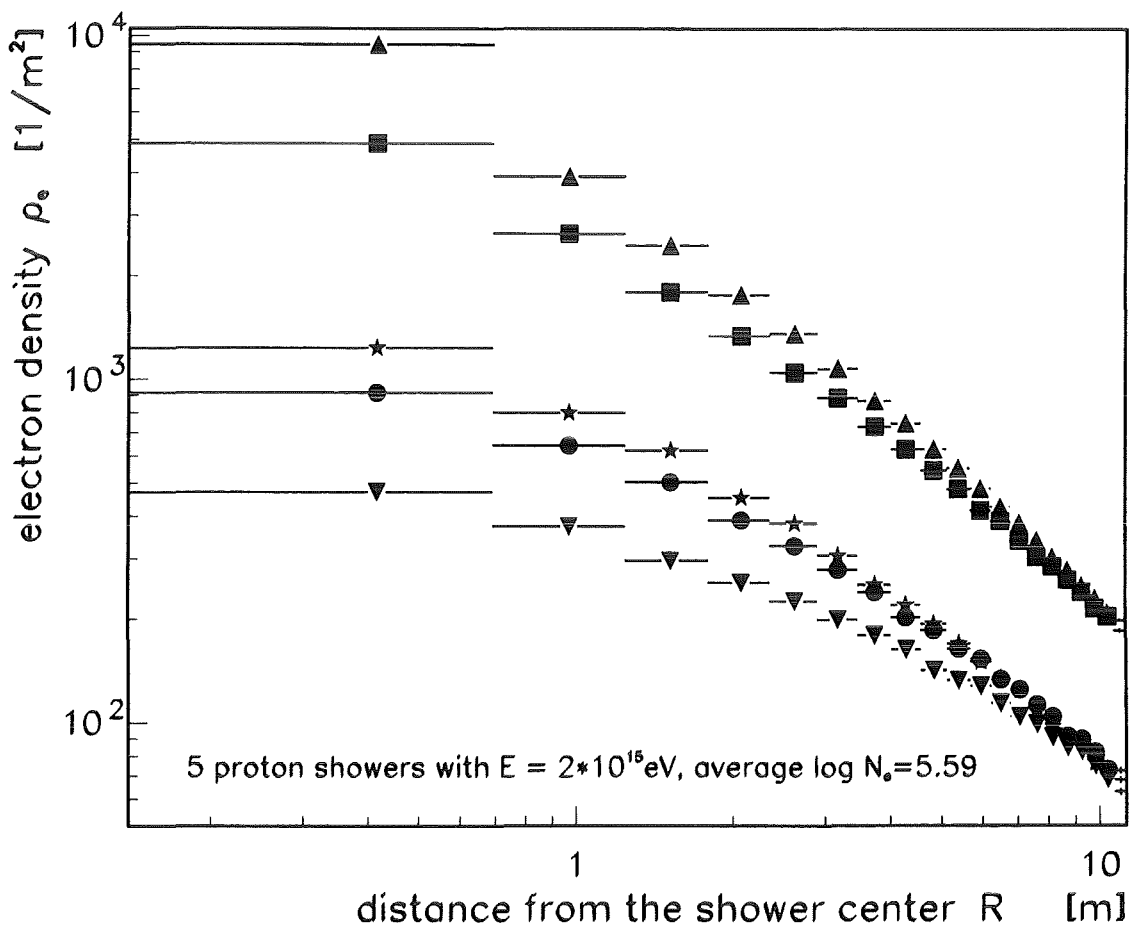
Figure A2: Electron density distributions of 5 individual proton induced showers, calculated by CORSIKA (EGS4).
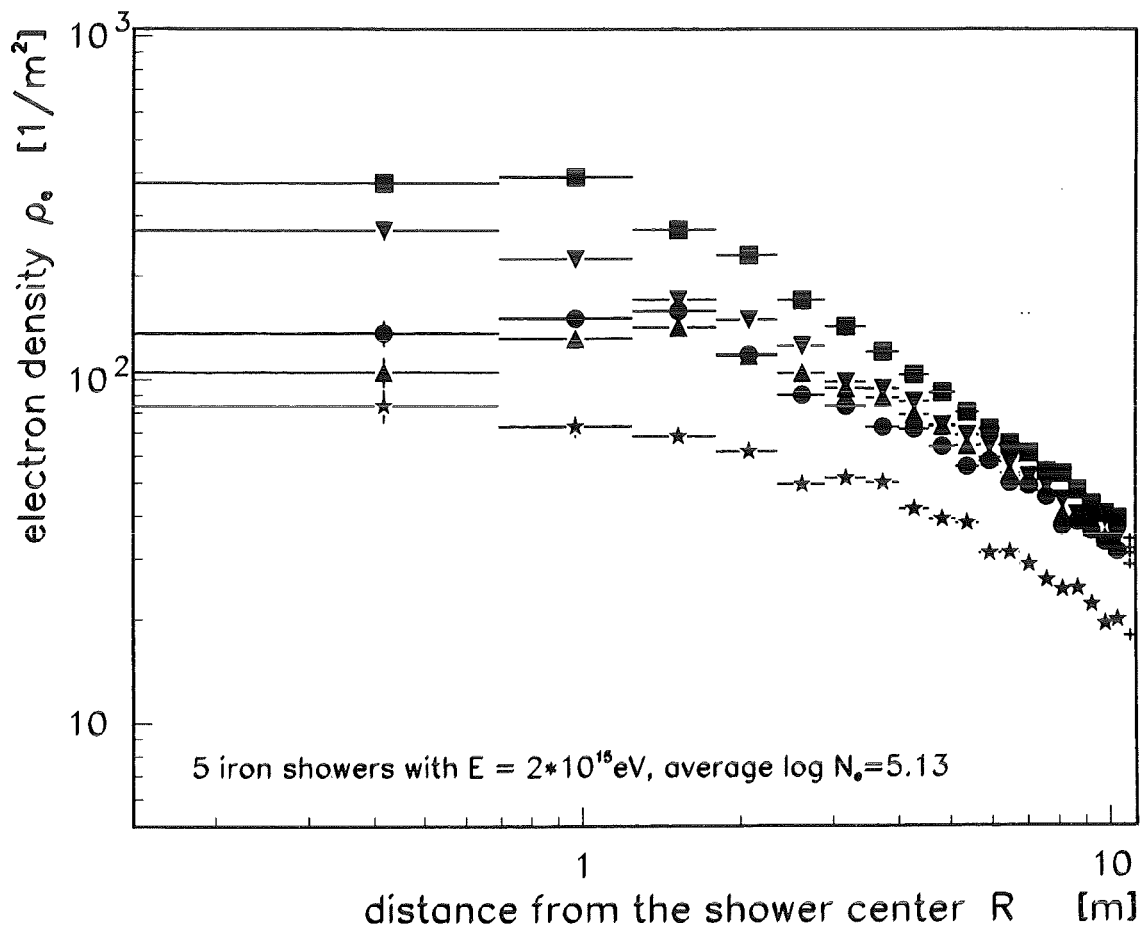
Figure A3: Electron density distributions of 5 individual iron induced showers, calculated by CORSIKA (EGS4).